Metallophysics and Advanced Technologies
Металофіз. новітні технол.
Metallofiz. Noveishie Tekhnol.
2026, vol. 48, No. 6, pp. 569–586
https://doi.org/10.15407/mfint.48.06.0569
Reprints available directly from the publisher

PACS numbers: 46.35.+z, 61.72.Bb, 61.72.Hh, 61.72.Lk, 62.20.fg, 83.10.Ff

Features of the Motion of the Critical Segment of Dislocation in a Multicomponent Alloy

M. I. Lugovy, D. G. Verbylo, M. P. Brodnikovskyy, T. I. Verbytska[*], D. S. Leonov[**], and M. Yu. Barabash[*,**,***]

I. M. Frantsevich Institute for Problems in Materials Science, N.A.S. of Ukraine,
3 Omeljan Pritsak Str.,
UA-03142 Kyiv, Ukraine
[*]*National Technical University of Ukraine*
'Igor Sikorsky Kyiv Polytechnic Institute',
37 Beresteiskyi Ave.,
UA-03056 Kyiv, Ukraine
[**]*Technical Centre, N.A.S. of Ukraine,*
13 Pokrovs'ka Str.,
UA-04070 Kyiv, Ukraine
[***]*Institute for Applied Control Systems, N.A.S. of Ukraine,*
42 Academician Hlushkov Ave.,
UA-03187 Kyiv, Ukraine

The motion of a critical segment of a dislocation in a field of stochastic shear stresses within the glide plane in a multicomponent alloy can be considered as one-dimensional motion of an effective point object to analyse thermal activation. However, such point objects should be regarded as under the influence of an effective one-dimensional distribution of shear stresses, the characteristics of which differ from the characteristics of a real two-dimensional distribution. A method for determining the characteristics of an effective distribution is proposed. Such distribution can be found by averaging the field of stochastic shear stresses over a characteristic region of the glide

Corresponding author: Maksym Yuriyovych Barabash
E-mail: mbarabash@nasu.kiev.ua

Citation: M. I. Lugovy, D. G. Verbylo, M. P. Brodnikovskyy, T. I. Verbytska, D. S. Leonov, and M. Yu. Barabash, Features of the Motion of the Critical Segment of Dislocation in a Multicomponent Alloy, *Metallofiz. Noveishie Tekhnol.*, **48**, No. 6: 569–586 (2026). DOI: 10.15407/mfint.48.06.0569

plane, which is a rectangle with dimensions equal to the length and height of the average bulge of the critical segment. It is possible because moving critical segments can be considered as 'smeared' ones over this characteristic region. Thus, the standard deviation and correlation length of an effective distribution can be determined from the known two-dimensional distribution. With the use of computer simulation, the dependence of the characteristics of the one-dimensional distribution on the characteristic averaging length is determined. As shown, the standard deviation of an effective distribution decreases and its correlation length increases with increasing averaging length, *i.e.*, the height of the average bulge. Therefore, the effective distribution has a smaller standard deviation and a longer correlation length compared to the corresponding characteristics of the field of stochastic shear stresses. The estimation of characteristics of effective distribution of shear stresses is important to analyse dislocation motion assisted with thermal activation in a multicomponent alloy.

Key words: multicomponent alloy, dislocation, shear stress, standard deviation, correlation length.

Для аналізи термічної активації рух критичного сеґмента дислокації у полі стохастичних зсувних напружень у площині ковзання у багатокомпонентному стопі можна розглядати як одновимірний рух деякого ефективного точкового об'єкта. Однак такі точкові об'єкти слід розглядати як такі, що знаходяться під впливом ефективного одновимірного розподілу зсувних напружень, характеристики якого відрізняються від характеристик реального двовимірного розподілу. Запропоновано методу визначення характеристик такого ефективного розподілу. Такий розподіл можна знайти шляхом усереднення поля стохастичних напружень зсуву по характерній області площини ковзання, яка являє собою прямокутник з розмірами, що дорівнюють довжині та висоті середньої опуклости критичного сеґмента. Це можливо, оскільки рухомі критичні сеґменти можна вважати «розмазаними» по цій характерній області. Таким чином, стандартний відхил і довжину кореляції ефективного розподілу можна визначити з відомого двовимірного розподілу. За допомогою комп'ютерного моделювання визначено залежність характеристик ефективного одновимірного розподілу від характерної довжини усереднення. Показано, що стандартний відхил ефективного розподілу зменшується, а його довжина кореляції збільшується зі збільшенням довжини усереднення, тобто висоти середньої опуклости. Отже, ефективний розподіл має менший стандартний відхил і більшу довжину кореляції порівняно з відповідними характеристиками поля стохастичних зсувних напружень. Оцінка характеристик ефективного одновимірного розподілу зсувних напружень є важливою для аналізи термоактивованого руху дислокацій у багатокомпонентному стопі.

Ключові слова: багатокомпонентний стоп, дислокація, зсувне напруження, стандартний відхил, довжина кореляції.

(Received 26 February, 2026; in final version, 13 March, 2026)

1. INTRODUCTION

In many cases, multicomponent alloys can be used at elevated temperatures, and then the temperature dependence of their yield point will be critical. This dependence is caused by the thermally activated motion of dislocations in the stochastic shear stress field in the glide plane generated by solute atoms. Since these materials are promising from the point of view of engineering applications [1, 2], a detailed study of such dependence remains relevant. Many works are devoted to the study of various aspects of solid solution strengthening, which is the basic mechanism for the formation of the mechanical behaviour of multicomponent alloys [3–26]. Modelling of dislocation motion provides great help in such studies. An important issue in this case remains the correct description of the stochastic shear stress field in the glide plane.

The main characteristics of such a stress field in a multicomponent alloy are four parameters: standard deviations and correlation lengths of its short- and long-wave components [27–29]. It should be noted that the main role for thermally activated motion is played by the short-wave component of the shear-stress field [30, 31]. The issues of crystal-lattice distortion, the yield strength of multicomponent alloys and its temperature dependence, together with the modelling of dislocation motion within the glide plane by the method of discrete dislocation dynamics, have been considered in many other works [32–38].

The classical approach to describing the thermally activated motion of a dislocation through a potential barrier or a corresponding force barrier is to consider the dislocation as a point object moving along one direction, where there is a certain distribution of potential energy and, accordingly, the force acting on this object [39, 40]. Since the motion of a dislocation does not occur as a whole, but rather in parts as the movement of individual critical segments by the formation and transformation of bulges on them [30, 31], the real object of the dislocation motion is its part, which occupies a certain area on the glide plane, *i.e.*, in reality, it is not at all a point object, to which a single co-ordinate corresponds. In addition, in the region of the glide plane, in which the critical segment of the dislocation is located, in a multicomponent alloy, there is not a single force, but a whole distribution of shear stresses, which are generated by solute atoms [27–29]. Thus, the motion of the critical segment in the glide plane is more likely a subject of modelling, for example, by the method of discrete dislocation dynamics. However, such modelling has its drawbacks, especially, in the case of multicomponent alloys, where we have a complex field of stochastic shear stresses in the glide plane. First, it is a very laborious and time-consuming process. In addition, such modelling does not make it possible to distinguish clearly the key parameters of the process and, therefore, it is quite difficult to generalize its results. In comparison, the simplified consideration of the dislocation motion as a one-dimensional motion of an effective point object has certain advantages. First, it is a significant reduction in time costs, *i.e.*, faster obtaining of results. Second, it is a clearer interpretation of these results and a simpler comparison of them with the classical approach. However, the consideration of such a point object also has its problems. Instead of a two-dimensional distribution of shear stresses on the glide plane, it is necessary to find a single effective force that will act on such an object or, more precisely, an effective one-dimensional distribution of shear stresses.

The goal of this work is to consider the motion of a critical dislocation segment in a multicomponent alloy as a one-dimensional motion of an effective point object for a known two-dimensional distribution of stochastic shear stresses in the glide plane to develop a method for determining the characteristics of the effective one-dimensional distribution of shear stresses that will act on such a point object, and to determine the dependence of the characteristics of the one-dimensional distribution on the characteristic averaging length using computer modelling.

2. CALCULATION ALGORITHMS

The critical segment of the dislocation, like the dislocation itself, cannot move in the glide plane as a whole without changing its shape. On the critical segments, bulges are formed, which, under the action of external stresses, begin to change their shape, and only this causes the segment to move in a certain direction. Each bulge is characterized by its height (the size of the bulge perpendicular to the dislocation line) and length (the size of the bulge along the dislocation line). It is clear that a large number of such bulges with various heights and lengths are formed on the dislocation line. Nevertheless, we can consider some averaged bulge, which will represent all other bulges. The determination of the parameters of such a bulge is considered in Ref. [36]. If we use the approximate bulge parameters found in this work for the Cr–Co–Ni–Fe–Mn alloy for certainty, we can show schematically the idealized process of movement of the averaged critical dislocation segment (Fig. 1). The main characteristic shapes and positions of the segment are depicted by solid black lines and are sequentially numbered. The grey lines show the intermediate shapes, which exist between the main shapes. The horizontal dashed lines show the average co-ordinates of the corresponding bulges. We assume that the segment movement occurs in the positive direction of the x axis, and the dislocation is located along the z axis. We will assume that there is initially a bulge *1* directed downwards against the direction of movement with a certain length and height at zero external stress. We can assign it the average co-ordinate $x = 0$. If we apply sufficient external stress, the bulge *1* will straighten to state *2*. The absolute height of the bulge under these con-

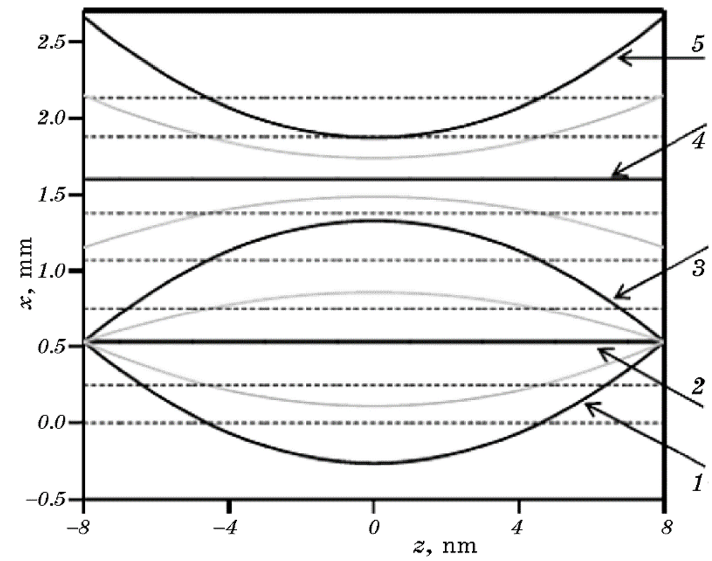

Fig. 1. Idealized process of movement of the averaged critical segment for the Cr–Co–Ni–Fe–Mn alloy.

ditions will decrease to zero with a constant length of the bulge. The average co-ordinate will increase. Further changes in the shape of the bulge will make it directed upwards in the direction of the segment movement. The absolute height will start to increase again, and the average co-ordinate will continue to increase. In the next step, the bulge will take shape *3*. Note that, in this part of the movement from shape *1* to shape *3*, the ends of the segment remain stationary, while the rest of its parts move. Next, the bulge goes from shape *3* (directed upwards) to shape *4* (straightened). The absolute height will then decrease to zero again; the average co-ordinate will increase. After shape *4*, the bulge will become again directed downwards, and the absolute height will start to increase again. From shape *4*, the bulge passes into shape *5*, which is a repetition of shape *1*. After that, the process is repeated. Note that, when moving from shape *3* to shape *5*, all parts of the segment move.

The change in the absolute height of the bulge with a change in the average co-ordinate of the critical segment is shown in Fig. 2. The numbers correspond to the numbers of the base shapes of the segment in Fig. 1. Periodic changes in the height of the bulge during the movement of the critical segment are visible. It is also possible to introduce the concept of the average height of the bulge.

The idealized process of movement of the averaged critical segment of a dislocation is a somewhat simplified representation of how the dislocation actually moves, but it clearly shows that different parts of the

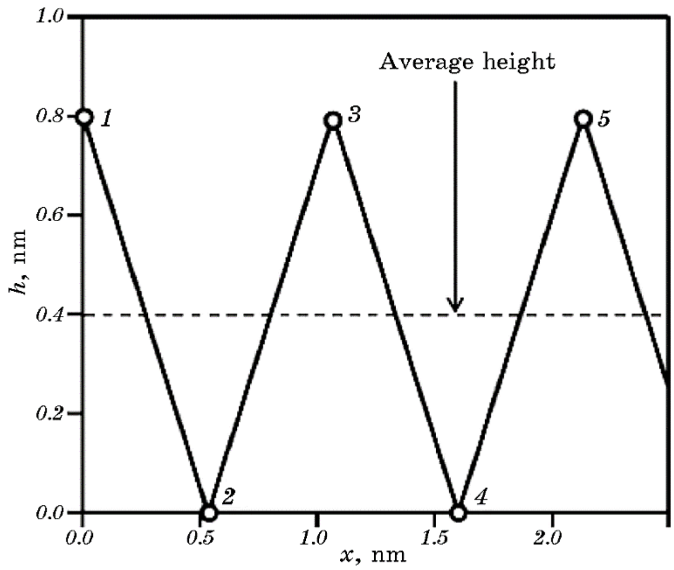

Fig. 2. Change in the absolute height of the bulge with a change in the average co-ordinate of the critical segment during the idealized movement process for the Cr–Co–Ni–Fe–Mn alloy.

segment at the same time occupy different positions on the glide plane. That is, a whole set of forces acts on the segment at each time point, not a single force. In addition, we considered this idealized process here also in order to demonstrate that the critical segment as a set of its individual parts with different co-ordinates at each time point can be characterized by a single average co-ordinate x. Moreover, the critical segment in the idealized process is averaged, that is, it represents effectively a whole set of real segments with different bulges. That is, some part of the averaged segment does not correspond in the idealized, simplified process, but, in reality, to a whole set of parts of real segments with different locations. Thus, the co-ordinates of such a part are to some extent uncertain. This gives reason to believe that it is possible to consider such an averaged segment as a 'smeared' one over a certain characteristic region of the glide plane. Moreover, this, in turn, suggests a way, in which such an object distributed over some two-dimensional region can be represented as a point object.

Considering an effective point object located in the centre of a characteristic region on the glide plane, where the critical segment is 'smeared', the effective force that will act on it is simply the force acting from the side of the field of stochastic shear stresses averaged over this characteristic region. We note that the linear tension forces of a two-dimensional segment, when averaged, give zero because the direction of action of these forces depends on where the bulge is directed, and the probabilities of bulges, which can be located in the characteristic region and directed 'down' or 'up', are the same. For every linear tension force directed 'downward', there will be necessarily a linear tension force of the same absolute magnitude directed 'upward'.

It is obvious that the simplest and most reasonable shape of the characteristic region is a rectangle (Fig. 3). The size of this rectangle along the z axis should be equal to the length of the averaged bulge L [36], and the question of its size $\lambda = h$ (the characteristic length of averaging) along the x axis is not so well defined, since the height of the bulge is variable in time, and the average length of the bulge is constant. It is possible to equate this size to the average height of the bulge within the first approximation, which is similar to that shown in Fig. 2 for the Cr–Co–Ni–Fe–Mn alloy, but it should be remembered that this figure shows the dependence for an idealized (simplified) process, so, a definition similar to that in Fig. 2 gives a rather inaccurate estimate of the average height. For rational reasons, this size is rather in the range from the average height as in Fig. 2 to the maximum height in this figure. The effective one-dimensional shear-stresses' distribution along the x axis ($z = 0$) for a point object representing a critical segment can be found by averaging the field of stochastic shear stresses over the characteristic region shown in Fig. 3:

$$< \tau_s(x) >= \frac{1}{A} \iint_A \tau_s(x, z) dA \,, \tag{1}$$

where $A = \lambda L$ is the area of the characteristic region, $\tau_s(x, z)$ is the distribution of stochastic shear stresses around the point with coordinates x and $z = 0$ on the slip plane, which can be determined by the method described in Refs. [27, 28]. The double integral (1) can be rewritten as a repeated integral, if we take into account the characteris-

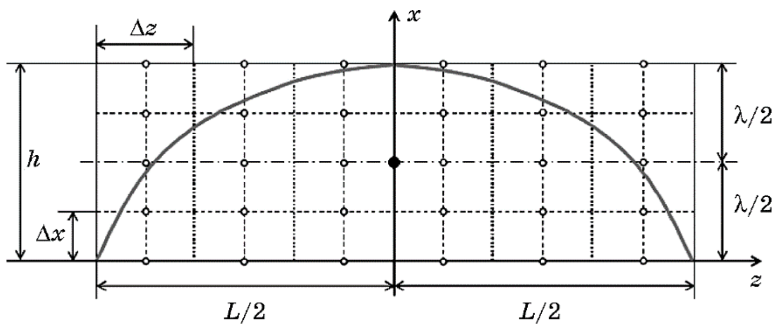

Fig. 3. Characteristic region on the glide plane, where the critical segment is 'smeared'. The black dot inside the rectangle represents the effective point object. The grey line shows one of the probable bulges of the critical segment, which fits into the characteristic region.

tic region, which is depicted in Fig. 3:

$$<\tau_s(x)> = \frac{1}{\lambda L}\int_{x-\lambda/2}^{x+\lambda/2}\left(\int_{-L/2}^{L/2}\tau_s(u,z)dz\right)du\,, \tag{2}$$

where u is the integration variable along the x axis.

Now, let us consider some features of the distribution of shear stresses $\tau(x, z)$, in order to determine the internal integral in the repeated integral (2). The calculation of stochastic shear stresses within the glide plane requires a rather significant amount of time and, therefore, these stresses are usually determined only at a finite number of points. Along the z axis, these points are spaced at a step Δz, which is usually not less than the correlation length of the shear-stress field. Thus, the stresses at these points along the z axis as random variables will be independent of each other. Along the x axis, these points are spaced at a step, which is usually less than the correlation length [27, 28]. When modelling, for example, by the method of discrete dislocation dynamics, it is also necessary to know the shear stresses at points along the x axis, which lie between the points, where the stresses are calculated using the method described in Refs. [27, 28]. In this case, linear interpolation is used. The stresses determined in this way also fit well to a normal distribution with the same parameters as the stresses calculated using the method described in Refs. [27, 28]. Thus, the distribution of shear stresses within the glide plane can be shown schematically as in Fig. 4. Shear stresses are defined on the glide plane in strips, which are parallel to the x axis and have a width Δz. With this definition, the inner integral in Eq. (2) can be replaced by a sum with stresses, which are defined for a single co-ordinate u along the x axis and with different co-ordinates z_i:

$$<\tau_s(x)> = \frac{1}{\lambda L}\int_{x-\lambda/2}^{x+\lambda/2}\left(\sum_{i=1}^{n_z}\tau_s(u,z_i)\Delta z\right)du\,, \tag{3}$$

where $n_z \approx L/\Delta z$. This is valid under the condition $L >> \Delta z$, which is usually fulfilled for critical dislocation segments in multicomponent alloys [36].

Recall that, in our conditions, the shear stresses at points along the z axis, which are located at a distance from each other not less than the correlation length of the shear-stress field, are actually independent normal random variables $\tau_s(u, z_i) = s(\Delta z)N(0, 1)$, where $s(\Delta z)$ is the standard deviation of the distribution of shear stresses in the glide plane, which is defined for the given Δz [27, 28], $N(0, 1)$ is the standard normal variable with zero mathematical expectation and a variance equal to one.

Then, the sum in Eq. (3) will be equal to

$$\sum_{i=1}^{n_z} \tau_s(u,z)\Delta z = \sum_{i=1}^{n_z} s(\Delta z)N(0,1)\Delta z = s(\Delta z)\Delta z N(0,n_z) = s(\Delta z)\sqrt{L\Delta z}N(0,1)\,, \quad (4)$$

that is, the sum will be a normal random variable with zero mathematical expectation and a standard deviation equal to $s(\Delta z)\sqrt{L\Delta z}$ and independent of the co-ordinate u along the x axis. Thus, the standard deviation $s(\Delta z)\sqrt{L\Delta z}$ can be taken out behind the integral sign. Note that the distributions of shear stresses in each strip parallel to the x axis (Fig. 4) have the same correlation length, and the distribution of the sum (4) along the x axis will have the same correlation length.

What in this case will remain under the integral sign in Eq. (3)? On the one hand, this is a standard normal variable $N(0, 1)$, but this is not enough for a complete definition and calculations. In practice, we will have certain numbers, which are given at points with co-ordinates x_i and $z = 0$ with a step Δx along the x axis. These numbers will have a standard normal distribution with zero mathematical expectation and a variance equal to one, *i.e.*, confirm that these are realizations $N(0, 1)$ at different points of the glide plane. In addition, the correlation length of the distribution of these numbers along the x axis will be equal to the correlation length of the shear-stresses' distribution in each strip parallel to the x axis. The simplest way to obtain the distribution of such numbers is to use the shear-stresses' distribution $\tau_s(x_j, 0)$, which is calculated for the given Δz by the method described in

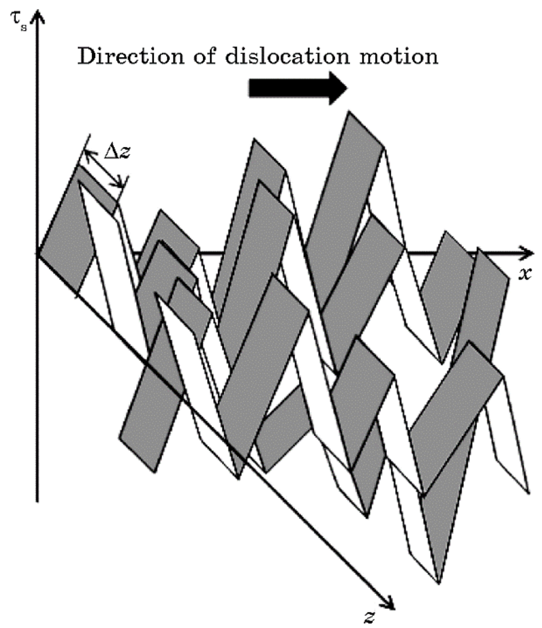

Fig. 4. Distribution of stochastic shear stresses within the glide plane.

Refs. [27, 28]. Such a distribution will have zero expectation and standard deviation $s(\Delta z)$ together with the necessary correlation length. If we divide each $\tau_s(x_j, 0)$ by $s(\Delta z)$ ($N_j = \tau_s(x_j, 0)/s(\Delta z)$), then, the expectation and correlation length of the distribution will not change, and the standard deviation will become equal to 1, which is required. The value at a point with the co-ordinate u along the x axis and the co-ordinate $z = 0$ in the interval between the points with the co-ordinates x_j and x_{j+1} ($z = 0$) can be calculated using linear interpolation:

$$N(u) = N_j + \frac{N_{j+1} - N_j}{x_{j+1} - x_j}(u - x_j), \tag{5}$$

where N_j is the number given at the point with co-ordinate x_j, N_{j+1} is the number given at the point with co-ordinate x_{j+1}; $x_{j+1} - x_j = \Delta x$. Thus, formula (3) becomes:

$$< \tau_s(x) >= \frac{s(\Delta z)}{\lambda}\sqrt{\frac{\Delta z}{L}}\int_{x-\lambda/2}^{x+\lambda/2} N(u)du\,, \tag{6}$$

If we calculate $<\tau_s(x)>$ along the x axis according to formula (6), then, for this averaged (smoothed) with a characteristic averaging length λ of the distribution, we can determine the zero mean value, as well as the standard deviation and the correlation length, which will differ from the standard deviation and the correlation length of the distribution $\tau_s(x_j, 0)$ [27, 28]. The correlation length was defined as the average length of segments along the corresponding distribution, where the stresses had the same sign, that is, were positive or negative within the boundaries of one segment [28, 35].

In the process of integration according to formula (6), the numbers $N(u)$ at points along the x axis, which lie between the points, where the stresses are calculated using the method described in Refs. [27, 28], are determined using linear interpolation. The numbers and their corresponding stresses calculated in this way also fit well into the normal distribution with the same parameters as the numbers and stresses calculated using the method described in Refs. [27, 28]. However, the stresses and the corresponding numbers $N(u)$ at intermediate points can also take other values, which are different from those calculated using linear interpolation. This will certainly affect the accuracy of the estimate of $<\tau_s(x)>$ using formula (6). The complexity of determining the stresses at intermediate points is because such a stress is a correlated random variable, the value of which will be random, on the one hand, and, on the other hand, will depend on the known values at neighbouring points. This problem is shown schematically in Fig. 5. The point B corresponds to the stress $\tau_i = \tau_s(x_j, 0)$ at the point A with co-ordinate x_j. The point D corresponds to the stress $\tau_{i+1} = \tau_s(x_{j+1}, 0)$ at the point E with

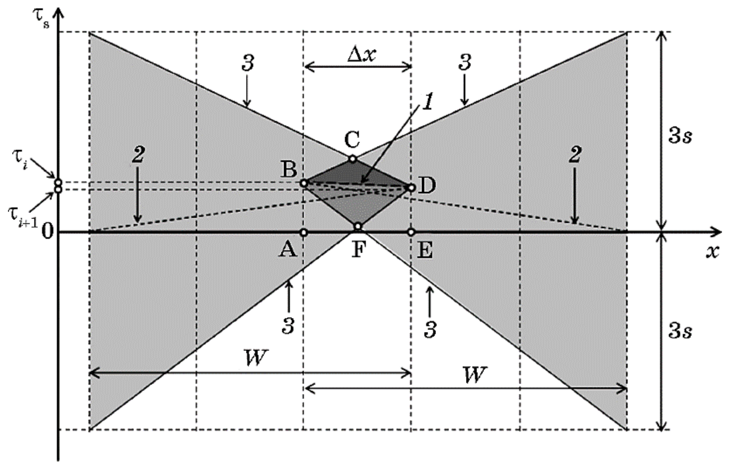

Fig. 5. Diagram showing the problem of determining stresses at intermediate points.

co-ordinate x_{j+1}.

The dotted line *1*, which connects B and D, shows the values, which can be found using linear interpolation. The values τ_i and τ_{i+1} in our consideration are not random, but given, that is, they can be conditionally considered as random variables with mathematical expectations τ_i and τ_{i+1}, and zero standard deviations. At a distance of the correlation length w and a greater distance to the right of the point A and to the left of the point E, the stresses become independent normal random variables with zero mathematical expectation and standard deviation s, such that almost all of their possible values lie in the range from $-3s$ to $+3s$. Closer to the points A and E, we have random variables, which are correlated with the values at the points A and E. We will consider them to be normally distributed with mathematical expectations and standard deviations, which depend on the distances to the points A and E, respectively.

Lines *2* show, within the first approximation, the mathematical expectations of such correlated random variables (Fig. 5). At points A and E, these mathematical expectations are equal to τ_i and τ_{i+1}, respectively, and, at a distance of the correlation length w and a greater distance to the right of the point A and to the left of the point E, these mathematical expectations are equal to zero. Lines *3* in Fig. 5 show, within the first approximation, the boundaries of the regions, in which lie almost all possible values of random variables, which are correlated with the values at points A and E, respectively. At the points A and E themselves, these regions have zero size, *i.e.*, zero standard deviations, and, at a distance of the correlation length w and a greater distance to the right of the point A and to the left of the point E, these regions extend from $-3s$ to $+3s$.

Between points A and E, the values are possible, which are correlated simultaneously with the values at both of these points. That is, almost all possible values of such correlated random variables must lie inside the quadrangle BCDF (Fig. 5). The most probable values will be on lines 2, but it is clearly seen that line *1* lies relatively close to these lines of most probable values. This explains that linear interpolation gives a good approximation for intermediate points. Nevertheless, the stresses and, accordingly, the numbers $N(u)$ at intermediate points can take other values, with a small probability even outside the quadrangle BCDF. In order to estimate the deviations of $<\tau_s(x)>$, to which these other values can cause, it is enough to analyse the results of integration according to formula (6), when $N(u)$ is determined not by linear interpolation along line *1*, but along broken lines BCD and BFD, respectively.

For line BCD,

$$N(u) = N_j + \frac{N_C - N_j}{x_C - x_j}(u - x_j),\; x_j \le u \le x_C\,, \tag{7a}$$

$$N(u) = N_C + \frac{N_{j+1} - N_C}{x_{j+1} - x_C}(u - x_C),\; x_C \le u \le x_{j+1}\,, \tag{7b}$$

where

$$N_C = \frac{\tau_i w + (3s - \tau_i)(x_C - x_j)}{s(\Delta z)w}, \tag{8a}$$

$$x_C = \frac{(\tau_{i+1} - \tau_i)w + (3s - \tau_i)x_j + (3s - \tau_{i+1})x_{j+1}}{6s - \tau_i - \tau_{i+1}}, \tag{8b}$$

For line BFD,

$$N(u) = N_j + \frac{N_F - N_j}{x_F - x_j}(u - x_j),\; x_j \le u \le x_F\,, \tag{9a}$$

$$N(u) = N_F + \frac{N_{j+1} - N_F}{x_{j+1} - x_F}(u - x_F),\; x_F \le u \le x_{j+1}\,, \tag{9b}$$

where

$$N_F = \frac{\tau_i w - (3s + \tau_i)(x_F - x_j)}{s(\Delta z)w}, \tag{10a}$$

$$x_F = \frac{(\tau_i - \tau_{i+1})w + (3s + \tau_i)x_j + (3s + \tau_{i+1})x_{j+1}}{6s + \tau_i + \tau_{i+1}}, \tag{10b}$$

Depending on the relative location of the points B and D, the regions, in which lie almost all possible values of the random variables, which are correlated with the values at the points A and E, respectively, may not intersect. Then, the region of possible values BCDF degenerates into a line *1*, which connects the points B and D. Then, almost all possible values between the points A and E, which are correlated simultaneously with the values at both of these points, will lie on this line.

3. RESULTS AND DISCUSSION

To verify the method of determining the characteristics of the effective one-dimensional distribution of shear stresses, which will act on a point object representing a critical segment of a dislocation in a field of stochastic shear stresses in the glide plane, a study of the influence of the characteristic averaging length λ on these characteristics was carried out using computer simulation. First, several distributions $\tau_s(x_j, 0)$ of shear stresses generated by solute atoms were calculated for a given $\Delta z = 2$ nm using the method described in Refs. [27, 28] for a multicomponent Cr–Co–Ni–Fe–Mn alloy. The initial parameters for modelling the shear-stress field in this alloy are given in Table 1. The shear stresses were calculated along the x axis at points with co-ordinates x from 0 to 125 nm with a step of $\Delta x = 0.125$ nm and a fixed co-ordinate $z = 0$. The calculated distributions had zero mathematical expectation, standard deviations $s(\Delta z) = 197$, 206, 210 MPa and correlation lengths $w = 0.41$, 0.4, 0.43 nm, respectively. The averaged bulge lengths L were calculated for our distributions using the technique described in Ref. [36]. These lengths were of 15, 14.6 and 14.4 nm, respectively. Second, for each distribution separately, we determined $N_j = \tau_s(x_j, 0)/s(\Delta z)$ at points with x_j. Third, each distribution $\tau_s(x_j, 0)$ was averaged separately according to formula (6) with different characteristic averaging lengths λ ranging from 0 to 1.25 nm, and the value $N(u)$ was determined using linear interpolation. The value $\lambda = 0$ corresponds to the absence of averaging along the x axis, *i.e.*, only averaging along the z axis is present. For each averaged distribution, its standard deviation s_λ and correlation length w_λ were found. In order to estimate the deviations $<\tau_s(x)>$, which may be caused by possible values $N(u)$, which do not correspond to linear interpolation, the integration was performed additionally according to formula (6), when $N(u)$ was determined not by linear interpolation, but along broken lines BCD

TABLE 1. Initial parameters for modelling the shear-stress field within the Cr–Co–Ni–Fe–Mn alloy [28].

G, GPa	K, GPa	ν	b, nm	V_a, nm^3
81	176	0.3	0.25	0.011

and BFD, accordingly, as described in the previous section.

The dependences of the relative standard deviations and correlation lengths of the averaged shear-stresses' distributions in the case, when the value $N(u)$ was determined by linear interpolation on the relative averaging length λ/w_0, are shown in Fig. 6. Each value s_λ and w_λ is divided into the corresponding values s_0 and w_0, for which $\lambda = 0$, for each averaged distribution. Therefore, for $\lambda/w_0 = 0$, we always have 1. In addition, we note that $s_0 = s(\Delta z)(\Delta z/L)^{1/2}$ and $w_0 = w$, since

$$\lim_{\lambda\to 0}\frac{1}{\lambda}\int_{x-\lambda/2}^{x+\lambda/2} N(u)du = \tau_s(x,0)/s(\Delta z),$$

and the standard deviation of this random variable is equal to 1. The dashed vertical line on the left corresponds to 1 and, on the right, to 2. These lines limit the range of the most probable values in the sense of effective averaging. The effective average height of the convexity of the critical segment is in this range. The standard deviation decreases, when the averaging length increases. The value is always less than 1, when the correlation length, on the other hand, increases, when the averaging length increases. The value is always equal to or greater than 1. The dashed vertical line on the left corresponds to $\lambda/w_0 = 1$ and, on the right, to $\lambda/w_0 = 2$. These lines limit the range of the most proba-

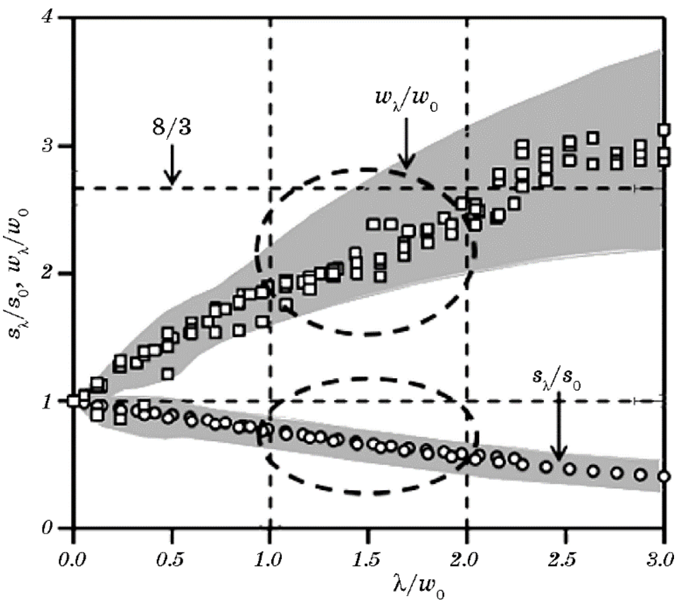

Fig. 6. Dependences of relative standard deviations and correlation lengths of averaged shear-stresses' distributions on the relative averaging length.

ble values of λ/w_0 in the sense of effective averaging $\tau_s(x_j, 0)$. The effective average height of the convexity of the critical segment is in this range. The standard deviation s_λ decreases, when the averaging length increases. The value s_λ/s_0 is always less than 1, when $\lambda/w_0 > 0$. The correlation length w_λ, on the other hand, increases, when the averaging length increases. The value w_λ/w_0 is always equal to or greater than 1.

We also add that the average values of all averaged shear-stresses' distributions obtained under the condition that the value $N(u)$ was determined by linear interpolation were close to zero that corresponds to a zero mathematical expectation. Integration according to formula (6), if $N(u)$ determined along the broken lines BCD and BFD and not by linear interpolation, leads to distributions with standard deviations and correlation lengths, which are close to the corresponding values in the case of linear interpolation, but the average values of these distributions are not close to zero. These average values are close to each other in absolute value, positive for the line BCD and negative for the line BFD. That is, they show a distribution shift, if we consider the values at intermediate points, which are greater than those ones calculated by linear interpolation (line BCD) and smaller than those calculated by linear interpolation (line BFD), and these shifts are close in absolute value. These biases can be used to estimate the inaccuracy of the calculation of the standard deviation s_λ of the averaged distribution. The upper bound s_λ^+ for the possible values s_λ can be estimated, if, in the corresponding averaged distribution calculated using linear interpolation, the mean value of the corresponding distribution for the line BCD is added to each positive value and the absolute value of the mean value of the corresponding distribution for the line BCD is subtracted from each negative value. The lower bound s_λ^- for the possible values s_λ can be estimated by subtracting from each positive value in the corresponding averaged distribution and adding to each negative value the absolute value of the mean value of the corresponding distribution for the line BFD. The results of the calculations, s_λ^+ / s_0 and s_λ^- / s_0, are shown in Fig. 6 as the upper and lower bounds of the grey band, in which the possible values s_λ/s_0 lie.

The inaccuracy of the standard deviation s_λ leads to the inaccuracy of the correlation length w_λ. The correlation length can be estimated by the formula $w = \pi s/s_g$, where s and s_g are the standard deviations of the shear stress and its gradient, respectively [29]. In our case, it will be $w_\lambda = \pi s_\lambda/s_g$. The standard deviation of the shear-stress gradient s_g is usually unknown, but, in the case, when we know w_λ, s_λ, the upper bound s_λ^+ of the standard deviation and its lower bound s_λ^-, we can estimate the upper bound w_λ^+ of the correlation length and its lower bound w_λ^-, assuming that s_g is the same for w_λ, w_λ^+ and w_λ^-. Then, we have $s_g = \pi s_\lambda/w_\lambda$, $w_\lambda^+ = w_\lambda s_\lambda^+ / s_\lambda$, and $w_\lambda^- = w_\lambda s_\lambda^- / s_\lambda$. The results of the calculations, w_λ^+ / w_0 and w_λ^- / w_0, are shown in Fig. 6 as the upper and lower bounds of the grey band, in which the possible values of w_λ/w_0 lie. This grey band expands quite strongly, *i.e.*, the accuracy of the determination decreases, when the averaging length increases.

In the range from $\lambda/w_0 = 1$ to $\lambda/w_0 = 2$, the relative average height of the critical segment bulge, *i.e.*, the effective relative averaging length to calculate the effective one-dimensional distribution of shear stresses, which will act on the point object representing the critical segment, lies. The relative standard deviation s_λ/s_0 varies from 0.46 to 0.88, and the relative correlation length w_λ/w_0 varies from 1.61 to 2.98 in this range of λ/w_0. Thus, the effective averaging gives the standard deviation $s_\lambda \approx 0.67s(\Delta z)(\Delta z/L)^{1/2}$ and $w_\lambda = 2.3w$. It is interesting to note that the expression for s_λ is very close in structure to the expression describing solid-solution hardening in Ref. [41]. In Ref. [39], an effective one-dimensional sinusoidal distribution of internal stresses was proposed for the analysis of thermally activated dislocation motion. An interesting point is that, for a given characteristic length w, at which the internal stresses have the same sign, the effective sinusoid in this work has a half-period $8w/3$, *i.e.*, 2.67 times longer than the real characteristic length. This is explained by the fact that a quarter of the sinusoid period (from 0 to the maximum stress) is associated with the transition of the critical segment from the convex shape *1* to the straight shape *2* as in Fig. 1. In this case, the average co-ordinate of the segment will change to $4w/3$, if shape *1* is a parabolic bulge with height $2w$. The half-period will then be $8w/3$, respectively. That is, this difference between the real and effective periods is due to the fact that the two-dimensional segment is averaged in a certain way. The result of our averaging, $w_\lambda = 2.3w$, is close to $8w/3$ from work [39].

4. CONCLUSION

The motion of a critical segment of dislocation in a field of stochastic shear stresses in a glide plane in a multicomponent alloy can be considered for the purpose of thermal activation analysis as a one-dimensional motion of an effective point object. However, such a point object should be considered under the action of an effective one-dimensional shear-stresses' distribution, the characteristics of which differ from the characteristics of the real two-dimensional distribution in the glide plane. The effective one-dimensional shear-stresses' distribution can be found by averaging the field of stochastic shear stresses over a characteristic area, which is a rectangle with dimensions equal to the length and height of the averaged bulge, since the critical segment of dislocation in the process of motion is as if 'smeared' one over this characteristic area of the glide plane. The standard deviation of the effective distribution decreases, and its correlation length increases with increasing averaging length, *i.e.*, the height of the averaged bulge. Therefore, the effective distribution has a smaller standard deviation and a longer correlation length compared to the corresponding characteristics of the stochastic shear-stress field in the glide plane. The evaluation of the characteristics of the effective one-dimensional shear-stresses' distribution is important for the analysis of thermally activated dislocation motion in a multicomponent alloy.

AUTHORS' CONTRIBUTIONS

M. I. Lugovy performed numerical calculations of shear-stress field in the glide plane and wrote the manuscript with input from all authors. D. G. Verbylo reviewed the literature and wrote the manuscript with input from all authors. M. P. Brodnikovskyy verified analytical approaches and provided critical feedback. T. I. Verbytska interpreted results and curated the data. D. S. Leonov validated, visualized, and verified results and prepared figures/tables. M. Yu. Barabash supervised the work and devised the main conceptual ideas. All authors approved the final version of the manuscript.

REFERENCES

1. D. B. Miracle and O. N. Senkov, *Acta Mater.*, **122**: 448 (2017).
2. E. P. George, W. A. Curtin, and C. C. Tasan, *Acta Mater.*, **188**: 435 (2020).
3. R. Labusch, *Czech. J. Phys. B*, **31**: 165 (1981).
4. L. A. Gypen and A. Deruyttere, *J. Mater. Sci.*, **12**, Iss. 5: 1028 (1977).
5. F. Otto, A. Dlouhy, Ch. Somsen, H. Bei, G. Eggeler, and E. P. George, *Acta Mater.*, **61**: 5743 (2013).
6. A. Gali and E. P. George, *Intermetallics*, **39**: 74 (2013).
7. S. J. Sun, Y. Z. Tian, H. R. Lin, X. G. Dong, Y. H. Wang, Z. J. Wang, and Z. F. Zhang, *J. Alloys Compd.*, **806**: 992 (2019).
8. A. V. Podolskiy, E. D. Tabachnikova, V. V. Voloschuk, V. F. Gorban, N. A. Krapivka, and S. A. Firstov, *Mater. Sci. Eng. A*, **710**: 136 (2018).
9. S. O. Firstov, T. G. Rogul, N. A. Krapivka, and S. I. Chugunova, *Metallofiz. Noveishie Tekhnol.*, **40**, No. 2: 219 (2018) (in Russian).
10. S. O. Firstov and T. G. Rogul, *Metallofiz. Noveishie Tekhnol.*, **39**, No. 1: 33 (2017) (in Russian).
11. M. Zaiser, *Phil. Mag. A*, **82**, Iss. 15: 2869 (2002).
12. J.-H. Zhai and M. Zaiser, *Mater. Sci. Eng. A*, **740–741**: 285 (2019).
13. G. Leyson, W. Curtin, L. Hector, and C. F. Woodward, *Nature Mater.*, **9**: 750 (2010).
14. G. P. M. Leyson, W. A. Curtin, L. G. Hector Jr., and Ch. F. Woodward, *Acta Mater.*, **60**: 3873 (2012).
15. G. P. M. Leyson and W. A. Curtin, *Modelling Simulation Mater. Sci. Eng.*, **24**: 065005 (2016).
16. C. Varvenne, A. Luque, and W. A. Curtin, *Acta Mater.*, **118**: 164 (2016).
17. C. Varvenne, G. P. M. Leyson, M. Ghazisaeidi, and W. A. Curtin, *Acta Mater.*,

124: 660 (2017).
18. G. Laplanche, J. Bonneville, C. Varvenne, W. A. Curtin, and E. P. George, *Acta Mater.*, **143**: 257 (2018).
19. W. G. Nöhring and W. A. Curtin, *Scripta Mater.*, **168**: 119 (2019).
20. G. Bracq, M. Laurent-Brocq, C. Varvenne, L. Perrière, W. A. Curtin, J.-M. Joubert, and I. Guillot, *Acta Mater.*, **177**: 266 (2019).
21. Y. Hu, B. A. Szajewski, D. Rodney, and W. A. Curtin, *Modelling Simulation Mater. Sci. Eng.*, **28**: 015005 (2020).
22. G. Péterffy, P. D. Ispánovity, M. E. Foster, X. Zhou, and R. B. Sills, *Mater. Theory*, **4**: 6 (2020).
23. R. Pasianot and D. Farkas, *Computational Mater. Sci.*, **173**: 109366 (2020).
24. J. D. Eshelby, *Solid State Physics*, **3**: 79 (1956).
25. R. L. Fleischer, *Acta Metallurgica*, **11**: 203 (1963).
26. I. Toda-Caraballo, *Scripta Mater.*, **127**: 113 (2017).
27. M. I. Lugovy, D. G. Verbylo, and M. P. Brodnikovskyy, *Uspikhy Materialoznavstva*, **3**: 24 (2021) (in Ukrainian).
28. M. I. Lugovy, D. G. Verbylo, and M. P. Brodnikovskyy, *Uspikhy Materialoznavstva*, **4–5**: 12 (2022) (in Ukrainian).
29. M. I. Lugovy, D. G. Verbylo, and M. P. Brodnikovskyy, *Uspikhy Materialoznavstva*, **7**: 3 (2023) (in Ukrainian).
30. M. I. Lugovy, D. G. Verbylo, and M. P. Brodnikovskyy, *Uspikhy Materialoznavstva*, **6**: 15 (2023) (in Ukrainian).
31. M. I. Lugovy, D. G. Verbylo, and M. P. Brodnikovskyy, *Metallofiz. Noveishie Tekhnol.*, **47**, No. 3: 303 (2025).
32. M. Lugovy, V. Slyunyayev, and M. Brodnikovskyy, *Prog. Natural Sci. Mater. Int.*, **31**: 95 (2021).
33. M. Lugovy, V. Slyunyayev, M. Brodnikovskyy, and S. O. Firstov, *Elektronnaya Mikroskopiya i Prochnost' Materialov*, **23**: 3 (2017) (in Ukrainian).
34. M. Lugovy, V. Slyunyayev, and M. Brodnikovskyy, *Elektronnaya Mikroskopiya i Prochnost' Materialov*, **25**: 26 (2019) (in Russian).
35. M. I. Lugovy, D. G. Verbylo, and M. P. Brodnikovskyy, *Uspikhy Materialoznavstva*, **2**: 19 (2021) (in Ukrainian).
36. M. I. Lugovy, D. G. Verbylo, and M. P. Brodnikovskyy, *Uspikhy Materialoznavstva*, **4/5**: 36 (2022) (in Ukrainian).
37. S. O. Firstov and T. G. Rogul, *Metallofiz. Noveishie Tekhnol.*, **44**, No. 1: 127 (2022) (in Ukrainian).
38. M. I. Lugovy, D. G. Verbylo, and M. P. Brodnikovskyy, *Uspikhy Materialoznavstva*, **8–9**: 13 (2024) (in Ukrainian).
39. A. S. Argon, *Strengthening Mechanisms in Crystal Plasticity* (Oxford: Oxford University Press: 2008).
40. U. F. Kocks, A. S. Argon, and M. F. Ashby, *Prog. Mater. Sci.*, **19**: 110 (1975).
41. F. R. N. Nabarro, *The Physics of Metals* (Ed. P. B. Hirsch) (Cambridge: Cambridge University Press: 1976), p. 152.